JACS
JOURNAL OF THE AMERICAN CHEMICAL SOCIETY
Article
Cite This: J. Am. Chem. Soc. 2019, 141, 643−647
pubs.acs.org/JACS

Chemical Requirement for Extracting Energetic Charge Carriers from Plasmonic Metal Nanoparticles to Perform Electron-Transfer Reactions

Vishal Govind Rao, Umar Aslam, and Suljo Linic*

Department of Chemical Engineering, University of Michigan, Ann Arbor, Michigan 48109, United States

Supporting Information

ABSTRACT: Performing electron-transfer reactions on metal nanoparticles requires separation of charge carriers at the nanoparticle and their transfer to the reacting molecules. Inducing these reactions using light is challenging due to the exceedingly short lifetimes of energetic charge carriers formed in metal nanoparticles under light illumination. The results described here show that certain conditions must be met to drive these electron-transfer reactions on plasmonic nanoparticles. One critical requirement is that the process of electronic excitation takes place at the nanoparticle/molecule interface. This is accomplished by high plasmonic electric fields at the surface of plasmonic nanoparticles. Furthermore, it is also evident from our study that the electron (or hole)-donating capacity of the hole (or electron) scavengers needs to be high enough to allow for the extraction of holes (or electrons) from the nanoparticle/molecule complex, therefore completing the catalytic cycle. We discuss these findings through a case study of the conversion of methylene blue (MB) into a reduced MB ion radical on the surface of plasmonic Ag and Ag−Pt core−shell nanoparticles. To directly monitor the reduction reaction of MB on the nanoparticle surfaces, we have used time-dependent *in situ* surface-enhanced Raman scattering measurement, which also informs us about the underlying mechanistic details of plasmon-driven charge transfer.

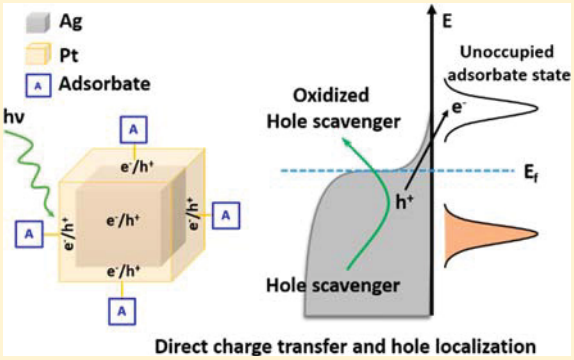

INTRODUCTION

Photocatalysis on plasmonic metallic nanostructures has received significant attention owing to the excellent light-trapping properties of localized surface plasmons and high chemical reactivity of metals.[1−5] The energy associated with the excitation of localized surface plasmon resonance (LSPR) can decay either radiatively through emission of photons or nonradiatively via the generation of energetic charge carriers within the nanoparticle.[6−8] These energetic charge carriers can drive photochemical reactions directly on the nanoparticle surface.[9−16] One mechanism by which these reactions can take place relies on transient exchange of hot charge carriers (Figure 1a) between the nanoparticle and the adsorbate (reactant). Transient excitation of hot carriers in the reactant results in vibrational heating of the reactant, which can then lead to a chemical reaction.[2,4] A critical feature of this "transient charge exchange" mechanism is that it does not require the extraction of charge carriers from the metal nanoparticles. Instead, the short-lived (femtoseconds lifetime)[17,18] transient excitation deposits energy into the reactant, which is sufficient to drive a reaction.[3,4,19,20]

Another question with significant ramifications in plasmonic catalysis is whether it is possible to move beyond the transient excitation by separating excited charge carriers and extracting them from photoexcited plasmonic metal nanoparticles to drive electron-transfer reactions in a manner that is mechanistically similar to classical photocatalytic reactions on semiconductors or molecular photocatalysts (Figure 1b). The

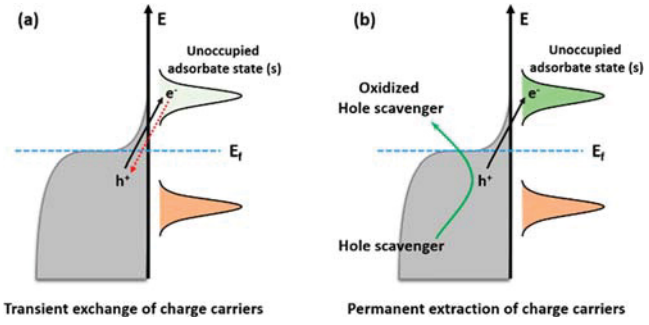

Figure 1. Illustration the light-induced charge carrier generation, excitation, and extraction mechanism on plasmonic nanoparticles. (a) Transient charge exchange mechanism in which the plasmon decays by directly exciting an electron into a hybrid unoccupied adsorbate state leaving a hole behind. The electron rapidly decays back to the nanoparticle (dotted red line indicates recombination). (b) Charge transfer in the presence of hole scavengers could lead to the permanent extraction of charge carriers, resulting in oxidation or reduction reactions.

Received: November 6, 2018
Published: December 11, 2018

DOI: 10.1021/jacs.8b11949
J. Am. Chem. Soc. 2019, 141, 643−647

principal issue that suggests that this might be difficult to accomplish is the ultrafast (femtoseconds, fs) decay (i.e., loss of energy) of energetic charge carriers in metal nanostructures.[17,21] We note that this short lifetime is a few orders of magnitude smaller than the lifetime of excited charge carriers in semiconductors and molecular photocatalysts.[22] This ultrafast decay suggests that before hot charge carriers can be extracted, they will relax in the metal, losing their energy.

Here we show an example of this charge extraction process, leading to electron-transfer reactions on plasmonic nanoparticles. By employing precisely tailored Ag nanocubes (~65 nm edge length) and Ag−Pt core−shell nanocubes, containing plasmonic Ag core nanocubes (Ag nanocubes ~65 nm edge length)[23] and a thin epitaxially grown Pt shell (~1.2 nm) entirely covering the cores[24,25] we shed light on the role of surface metal electronic structure in these charge extraction processes and reactions (see the Supporting Information for details of nanoparticle synthesis, characterization, extinction spectra, and TEM image). Furthermore, we analyze the role of chemical charge scavengers in these reactions. We show that the charge extraction process (i.e., the electron transfer reactions) requires direct resonant electronic excitation at the adsorbate on the metal surface[26,27] and the use of potent hole (or electron) scavengers that can efficiently relay charge, enabling charge separation and the electron-transfer reaction.[28−36] We demonstrate this in a case study of the photochemical, one-electron reduction of methylene blue (MB) to form MB ion radical in the presence of hole scavengers on Ag and Ag−Pt plasmonic nanoparticles.

■ DISCUSSION

We have previously shown that when MB is in contact with plasmonic Ag nanoparticles, direct electronic excitations can take place at the MB/Ag interface at some light wavelengths and not at others.[37,38] Our analysis showed that this process of charge excitation (leading to energetic charge carriers in MB) involves electronic states associated with the MB/Ag interface, where the electric fields are very high due to LSPR.[37,38] For example, this charge excitation process takes place when the MB/Ag system is illuminated by a 785 nm laser, as manifested by very high anti-Stokes/Stokes Raman intensity ratios.[37,38] The Raman spectra of the MB/Ag sample at pH 7 is shown in Figure 2a,b (see the Supporting Information for sample preparation/characterization details; Figures S1−S3, as well as for the corrections used for anti-Stokes and Stokes surface-enhanced Raman scattering (SERS) intensities to account for the Raman detector sensitivity and the wavelength-dependent electromagnetic enhancement). The measured high anti-Stokes to Stokes ratio at 785 nm excitation (Figure 2b) is the consequence of hot charge carriers transiently populating the MB molecule (Figure S4 further substantiates the role of charge transfer toward higher anti-Stokes to Stokes ratio at 785 nm excitation).[37,38] This transient charge transfer leads to the heating of the vibrational modes of MB, which manifests itself in high anti-Stokes scattering intensities. Interestingly, we found that this process of charge carrier exchange was not observed when we used a 532 nm Raman laser (Figure 2a). We stress that the high MB anti-Stokes SERS intensity with 785 nm excitation cannot be explained by the role of electromagnetic SERS enhancement, and its explanation requires that the energetic charge is exchanged at the MB/Ag interface.[37,38]

The SERS data of the MB/Ag−Pt sample at pH 7 is shown in Figure 2c,d. The charge exchange process occurs for MB in

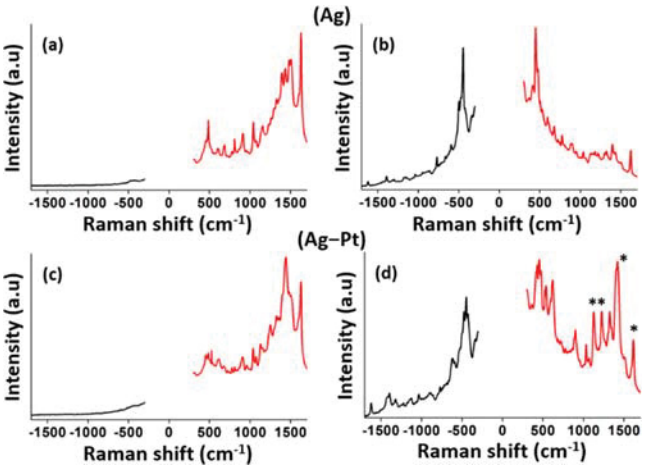

Figure 2. Surface-enhanced Raman spectra (SERS) showing anti-Stokes (black) and Stokes (red) spectra for MB/Ag samples at pH 7 collected using (a) 532 nm laser and (b) 785 nm laser and for MB/Ag−Pt samples at pH 7 collected using (c) 532 nm laser and (d) 785 nm laser. The marked peaks show the characteristic Raman peaks corresponding to the reduced form of MB.[39,40]

contact with the Ag−Pt core−shell nanoparticles at pH 7 for the 785 nm wavelength (Figure 2d) and not for the 532 nm wavelength (Figure 2c). The data in Figure 2d show that, unlike for MB on Ag, the Raman spectra for MB on Ag−Pt show features that resemble a reduced form of MB; that is, on the Pt surface the process of charge exchange is accompanied by one-electron reduction of MB to produce MB ion radical.[39,40]

The data in Figure 3 show the time-dependent SERS spectra for the MB/Ag (Figure 3a−c) and MB/Ag−Pt (Figure 3d−f) samples at pH 7 obtained with the 785 nm laser excitation. It is clear that the SERS spectrum for the MB/Ag sample remains unchanged over time. On the other hand, for the MB/Ag−Pt sample some peaks disappear and shift to new frequencies. In

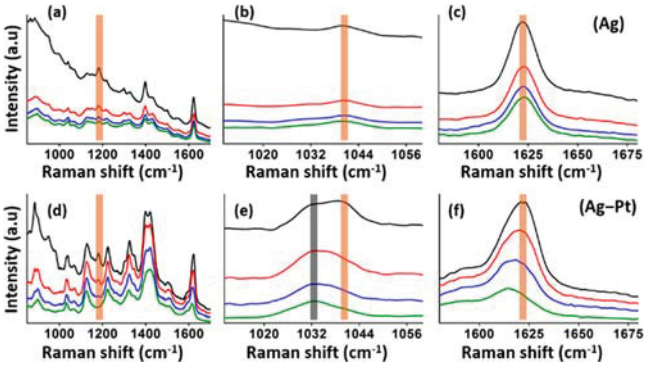

Figure 3. *In situ* SERS spectra monitoring time-dependent photocatalytic reaction of MB on Ag and Ag−Pt surfaces at pH 7, under 785 nm CW laser excitation. (a−c) Stokes spectra for MB/Ag samples collected at different time intervals (black: 1 min, red: 3 min, blue: 5 min, and green: 7 min): there is no observable shift in any Raman peak with time, which suggests that the reduction of MB does not occur on Ag nanoparticles. (d−f) Stokes spectra for MB/Ag−Pt samples collected at different time intervals (black: 1 min, red: 3 min, blue: 5 min, and green: 7 min): the peak at 1181 cm^{-1} disappears with time, the peak at 1040 cm^{-1} shifts to 1034 cm^{-1}, and the peak at 1622 cm^{-1} shifts to 1614 cm^{-1} with time, which confirms the reduction of MB on Ag−Pt nanoparticles.

DOI: 10.1021/jacs.8b11949
J. Am. Chem. Soc. 2019, 141, 643−647

particular, the peak at 1181 cm^{-1} diminishes with time, the peak at 1040 cm^{-1} shifts to 1034 cm^{-1}, and the peak at 1622 cm^{-1} shifts to 1614 cm^{-1}. All these spectral changes are consistent with the reduction of MB and the formation of the reduced ion radical form of MB.[39,40] We also observe that under identical experimental conditions, illumination with the 532 nm laser does not lead to an observable shift in any Raman peak with time (Figure S5), which indicates that MB does not react on either Ag or Ag−Pt nanoparticles at 532 nm excitation, suggesting a light of specific wavelength is required for the reaction to occur.

The data in Figure 3 show that the process of direct charge excitation at 785 nm for MB on Ag−Pt is accompanied by the charge extraction from the nanoparticle (i.e., an electron-transfer reaction) and the formation of the MB ion radical; however, under similar conditions for MB on Ag nanoparticles, this process does not occur. We hypothesized that this may be a result of the difference in the energy of charge carriers that are involved in the process of charge excitation and extraction on the two different materials (Ag and Ag−Pt nanoparticles). In particular, we postulated that the energetic holes generated during transient charge excitation on MB/Ag−Pt samples are of higher energy (further below the Fermi level) than the holes created in the MB/Ag samples (Figure 4). This difference in

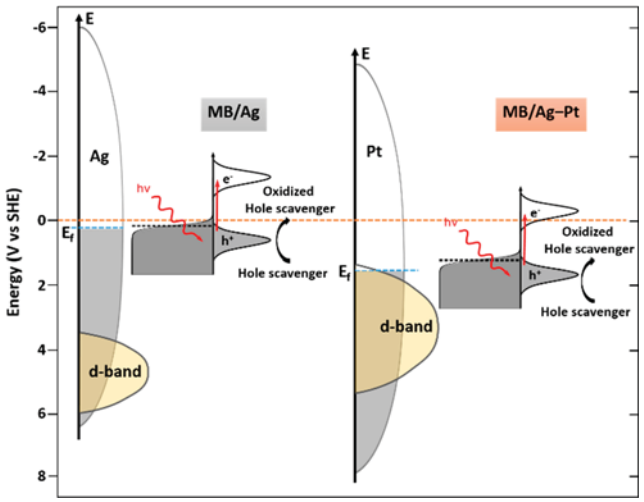

Figure 4. Schematic energy diagram showing simplified band structure for Ag and Pt metals and the probable relative energy for holes generated during charge excitation on MB/Ag and MB/Ag−Pt samples.

energy could lead to an increased likelihood of holes being scavenged by hydroxide anions on the MB/Ag−Pt nanoparticle, thereby enabling the MB reduction. Our hypothesis is based on the fact that in the case of the monometallic Ag nanoparticles, the Ag s states around the Fermi level are involved in the electronic excitations. These electronic excitations produce hot electrons and holes of approximately equal energies.[7,8] For the Pt surface of the Ag−Pt nanocubes, hot charge carriers are produced primarily through d-to-s interband excitation, which are generally believed to produce relatively high energy holes (Figure 4).[14]

To test this hypothesis, we performed time-dependent *in situ* SERS measurements for MB on Ag and Ag−Pt nanoparticles under different pH conditions (i.e., different concentrations of OH^-) (Figure 5). By changing the pH we effectively change

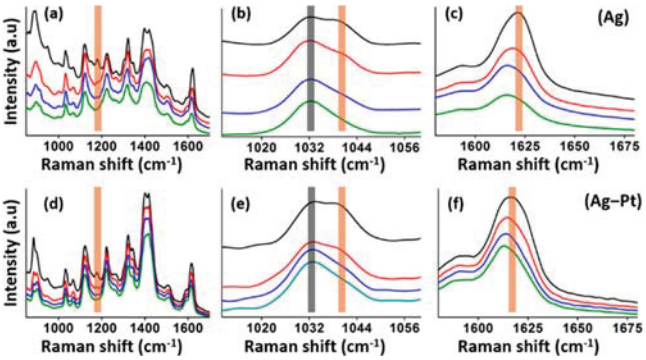

Figure 5. *In situ* SERS spectra monitoring time-dependent photocatylic reaction of MB on Ag and Ag−Pt surface at pH 12, under 785 nm CW laser excitation. (a−c) Stokes spectra for MB on Ag NC collected at different time intervals (black: 1 min, red: 3 min, blue: 5 min, and green: 7 min). (d−f) Stokes spectra for MB on Ag−Pt NC collected at different time intervals (black: 1 min, red: 3 min, blue: 5 min, and green: 7 min). For both MB on Ag and MB on Ag−Pt NC the peak at 1181 cm^{-1} (a and d) associated with MB disappears with time, the peak at 1040 cm^{-1} shifts to 1034 cm^{-1} (b, e), and the peak at ∼1622 cm^{-1} shifts to ∼1614 cm^{-1} (c, f) with time, which suggests that the reduction of MB occurs on both Ag and Ag−Pt NC at pH 12.

the free energy of the OH^- scavenger.[30,31] At higher pH, lower energy holes (closer to the Fermi level) can be extracted from the metal. Data in Figure 5a−c show that at pH 12 and above the reduction of MB can take place even on Ag nanoparticles, with the 785 nm laser excitation. It is noteworthy that even at pH 12 the reduction of MB does not occur with 532 nm laser excitation on either Ag or Ag−Pt nanoparticles (Figure S6).

We further tested this hypothesis by employing more potent hole scavengers than OH^-. Data in Figure 6 show that the

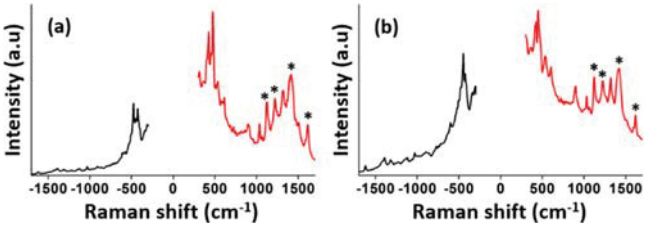

Figure 6. SERS spectra showing anti-Stokes (black) and Stokes (red) spectra for MB on Ag samples under 785 nm laser excitation in the presence of (a) sodium oxalate and (b) potassium acetate as hole scavengers. The marked peaks show the characteristic Raman peaks corresponding to the reduced form of MB,[39,40] which appear in the presence of a hole scavenger. Moreover, irrespective of hole scavenger used, similar Raman peaks for the reduced form of MB are observed.

presence of acetate and oxalate hole scavengers leads to the reduction of MB even at pH 7 on the Ag nanoparticles under resonant 785 nm excitation. Moreover, neither of the hole scavengers facilitate reduction at 532 nm excitation. These data are completely consistent with the experiments performed using hydroxide anions as the hole scavengers where the higher free energy of the electron-donating (hole-accepting) state of the hole scavengers yields higher reaction rates.

Collectively these measurements suggest that electron-transfer reactions on plasmonic nanostructures require that the process of charge excitation take place at the molecule−nanoparticle complex. In this particular example, the process of charge excitation only takes place under 785 nm excitation and

DOI: 10.1021/jacs.8b11949
J. Am. Chem. Soc. 2019, 141, 643−647

not under 532 nm excitation. Furthermore, it is also clear that the electron-donating capacity of the hole scavenger needs to be high enough to allow for the extraction of holes from the molecule−nanoparticle complex and therefore the completion of the catalytic cycle.

■ CONCLUSIONS

In summary, we have demonstrated that performing electron-transfer reactions on plasmonic metal surfaces requires electronic charge exchange between the nanoparticle and molecules as well as the use of relatively potent charge carrier scavengers. Our results indicate that the plasmonic nanoparticle serves multiple functions in these systems. On one hand, its interaction with a reacting molecule changes the electronic structure of the molecule via the creation of interfacial electronic states, which can be instrumental in LSPR-mediated electronic excitations. In this particular case the electronic excitation in the MB/nanoparticle complexes takes place at 785 nm, which is significantly lower energy than required for the optical excitation in independent MB molecules (~660 nm). The nanoparticle also plays an instrumental role in harvesting the energy of light and driving these electronic excitations at the molecule/nanoparticle interface via very high electric fields that are created at the LSPR frequencies.[37,38] Also, by changing the nature of the sites at the surface of the nanoparticles[41,42] (in this case the Ag versus Pt sites), it is possible to tune the energy of generated energetic electrons and holes so that different charge carrier scavengers can be used. Finally, by changing the nature of the surface sites, it should, in principle, be possible to involve different sites on the molecule (by controlling the way that molecules attach to the surface) and affect which groups on the molecule react.[43]

■ ASSOCIATED CONTENT

Supporting Information

The Supporting Information is available free of charge on the ACS Publications website at DOI: 10.1021/jacs.8b11949.

Details of nanoparticle synthesis and their characterization, extinction spectra, TEM image, Raman sample preparation, SERS data, information about SERS background correction, and additional references (PDF)

■ AUTHOR INFORMATION

Corresponding Author

*linic@umich.edu

ORCID

Vishal Govind Rao: 0000-0003-1205-3006

Umar Aslam: 0000-0001-8310-2958

Suljo Linic: 0000-0003-2153-6755

Notes

The authors declare no competing financial interest.

■ ACKNOWLEDGMENTS

This work was primarily supported by the National Science Foundation (NSF) (CBET-1702471 and CHE-1800197). The synthesis was developed with the support of the U.S. Department of Energy, Office of Basic Energy Science, Division of Chemical Sciences (FG-02-05ER15686). Secondary support for the development of analytical tools used to analyze the optical measurements was provided by the NSF (CBET-1436056). S.L. also acknowledges the partial support of the Technische Universität München, Institute for Advanced Study, funded by the German Excellence Initiative and the European Union Seventh Framework Programme under Grant Agreement No. 291763.

■ REFERENCES

(1) Zhang, Y.; He, S.; Guo, W.; Hu, Y.; Huang, J.; Mulcahy, J. R.; Wei, W. D. Surface-Plasmon-Driven Hot Electron Photochemistry. *Chem. Rev.* **2018**, *118* (6), 2927−2954.

(2) Christopher, P.; Xin, H.; Linic, S. Visible-Light-Enhanced Catalytic Oxidation Reactions on Plasmonic Silver Nanostructures. *Nat. Chem.* **2011**, *3* (6), 467.

(3) Mukherjee, S.; Libisch, F.; Large, N.; Neumann, O.; Brown, L. V.; Cheng, J.; Lassiter, J. B.; Carter, E. A.; Nordlander, P.; Halas, N. J. Hot Electrons Do the Impossible: Plasmon-Induced Dissociation of H2 on Au. *Nano Lett.* **2013**, *13* (1), 240−247.

(4) Christopher, P.; Xin, H.; Marimuthu, A.; Linic, S. Singular Characteristics and Unique Chemical Bond Activation Mechanisms of Photocatalytic Reactions on Plasmonic Nanostructures. *Nat. Mater.* **2012**, *11* (12), 1044.

(5) Dionne, J. A.; Baldi, A.; Baum, B.; Ho, C.-S.; Janković, V.; Naik, G. V.; Narayan, T.; Scholl, J. A.; Zhao, Y. Localized Fields, Global Impact: Industrial Applications of Resonant Plasmonic Materials. *MRS Bull.* **2015**, *40* (12), 1138−1145.

(6) Hartland, G. V.; Besteiro, L. V.; Johns, P.; Govorov, A. O. What's so Hot about Electrons in Metal Nanoparticles? *ACS Energy Lett.* **2017**, *2* (7), 1641−1653.

(7) Bernardi, M.; Mustafa, J.; Neaton, J. B.; Louie, S. G. Theory and Computation of Hot Carriers Generated by Surface Plasmon Polaritons in Noble Metals. *Nat. Commun.* **2015**, *6*, 7044.

(8) Sundararaman, R.; Narang, P.; Jermyn, A. S.; Iii, W. A. G.; Atwater, H. A. Theoretical Predictions for Hot-Carrier Generation from Surface Plasmon Decay. *Nat. Commun.* **2014**, *5*, 5788.

(9) Zhang, X.; Chen, Y. L.; Liu, R.-S.; Tsai, D. P. Plasmonic Photocatalysis. *Rep. Prog. Phys.* **2013**, *76* (4), 046401.

(10) Baffou, G.; Quidant, R. Nanoplasmonics for Chemistry. *Chem. Soc. Rev.* **2014**, *43* (11), 3898−3907.

(11) Marimuthu, A.; Zhang, J.; Linic, S. Tuning Selectivity in Propylene Epoxidation by Plasmon Mediated Photo-Switching of Cu Oxidation State. *Science* **2013**, *339* (6127), 1590−1593.

(12) Sprague-Klein, E. A.; McAnally, M. O.; Zhdanov, D. V.; Zrimsek, A. B.; Apkarian, V. A.; Seideman, T.; Schatz, G. C.; Van Duyne, R. P. Observation of Single Molecule Plasmon-Driven Electron Transfer in Isotopically Edited 4,4′-Bipyridine Gold Nanosphere Oligomers. *J. Am. Chem. Soc.* **2017**, *139* (42), 15212−15221.

(13) Linic, S.; Christopher, P.; Ingram, D. B. Plasmonic-Metal Nanostructures for Efficient Conversion of Solar to Chemical Energy. *Nat. Mater.* **2011**, *10* (12), 911−921.

(14) Zhang, L.; Jia, C.; He, S.; Zhu, Y.; Wang, Y.; Zhao, Z.; Gao, X.; Zhang, X.; Sang, Y.; Zhang, D.; et al. Hot Hole Enhanced Synergistic Catalytic Oxidation on Pt-Cu Alloy Clusters. *Adv. Sci. Weinh. Baden-Wurtt. Ger.* **2017**, *4* (6), 1600448.

(15) Christopher, P.; Moskovits, M. Hot Charge Carrier Transmission from Plasmonic Nanostructures. *Annu. Rev. Phys. Chem.* **2017**, *68* (1), 379−398.

(16) Aslam, U.; Rao, V. G.; Chavez, S.; Linic, S. Catalytic Conversion of Solar to Chemical Energy on Plasmonic Metal Nanostructures. *Nat. Catal.* **2018**, *1* (9), 656−665.

(17) Brown, A. M.; Sundararaman, R.; Narang, P.; Goddard, W. A.; Atwater, H. A. Nonradiative Plasmon Decay and Hot Carrier Dynamics: Effects of Phonons, Surfaces, and Geometry. *ACS Nano* **2016**, *10* (1), 957−966.

(18) Clavero, C. Plasmon-Induced Hot-Electron Generation at Nanoparticle/Metal-Oxide Interfaces for Photovoltaic and Photocatalytic Devices. *Nat. Photonics* **2014**, *8* (2), 95.

DOI: 10.1021/jacs.8b11949
J. Am. Chem. Soc. 2019, 141, 643−647

(19) Kazuma, E.; Jung, J.; Ueba, H.; Trenary, M.; Kim, Y. Direct Pathway to Molecular Photodissociation on Metal Surfaces Using Visible Light. *J. Am. Chem. Soc.* **2017**, *139* (8), 3115−3121.
(20) Kale, M. J.; Avanesian, T.; Christopher, P. Direct Photocatalysis by Plasmonic Nanostructures. *ACS Catal.* **2014**, *4* (1), 116−128.
(21) Manjavacas, A.; Liu, J. G.; Kulkarni, V.; Nordlander, P. Plasmon-Induced Hot Carriers in Metallic Nanoparticles. *ACS Nano* **2014**, *8* (8), 7630−7638.
(22) Ghosh, H. N.; Asbury, J. B.; Weng, Y.; Lian, T. Interfacial Electron Transfer between $Fe(II)(CN)_6^{4-}$ and TiO2 Nanoparticles: Direct Electron Injection and Nonexponential Recombination. *J. Phys. Chem. B* **1998**, *102* (50), 10208−10215.
(23) Van Cleve, T.; Gibara, E.; Linic, S. Electrochemical Oxygen Reduction Reaction on Ag Nanoparticles of Different Shapes. *ChemCatChem* **2016**, *8* (1), 256−261.
(24) Aslam, U.; Chavez, S.; Linic, S. Controlling Energy Flow in Multimetallic Nanostructures for Plasmonic Catalysis. *Nat. Nanotechnol.* **2017**, *12* (10), 1000.
(25) Aslam, U.; Linic, S. Addressing Challenges and Scalability in the Synthesis of Thin Uniform Metal Shells on Large Metal Nanoparticle Cores: Case Study of Ag−Pt Core−Shell Nanocubes. *ACS Appl. Mater. Interfaces* **2017**, *9* (49), 43127−43132.
(26) Kale, M. J.; Avanesian, T.; Xin, H.; Yan, J.; Christopher, P. Controlling Catalytic Selectivity on Metal Nanoparticles by Direct Photoexcitation of Adsorbate−Metal Bonds. *Nano Lett.* **2014**, *14* (9), 5405−5412.
(27) Wu, K.; Chen, J.; McBride, J. R.; Lian, T. Efficient Hot-Electron Transfer by a Plasmon-Induced Interfacial Charge-Transfer Transition. *Science* **2015**, *349* (6248), 632−635.
(28) Wu, K.; Chen, Z.; Lv, H.; Zhu, H.; Hill, C. L.; Lian, T. Hole Removal Rate Limits Photodriven H2 Generation Efficiency in CdS-Pt and CdSe/CdS-Pt Semiconductor Nanorod−Metal Tip Heterostructures. *J. Am. Chem. Soc.* **2014**, *136* (21), 7708−7716.
(29) Strmcnik, D.; Uchimura, M.; Wang, C.; Subbaraman, R.; Danilovic, N.; van der Vliet, D.; Paulikas, A. P.; Stamenkovic, V. R.; Markovic, N. M. Improving the Hydrogen Oxidation Reaction Rate by Promotion of Hydroxyl Adsorption. *Nat. Chem.* **2013**, *5* (4), 300.
(30) Kalisman, P.; Nakibli, Y.; Amirav, L. Perfect Photon-to-Hydrogen Conversion Efficiency. *Nano Lett.* **2016**, *16* (3), 1776−1781.
(31) Simon, T.; Bouchonville, N.; Berr, M. J.; Vaneski, A.; Adrović, A.; Volbers, D.; Wyrwich, R.; Döblinger, M.; Susha, A. S.; Rogach, A. L.; et al. Redox Shuttle Mechanism Enhances Photocatalytic H_2 Generation on Ni-Decorated CdS Nanorods. *Nat. Mater.* **2014**, *13* (11), 1013.
(32) Acharya, K. P.; Khnayzer, R. S.; O'Connor, T.; Diederich, G.; Kirsanova, M.; Klinkova, A.; Roth, D.; Kinder, E.; Imboden, M.; Zamkov, M. The Role of Hole Localization in Sacrificial Hydrogen Production by Semiconductor−Metal Heterostructured Nanocrystals. *Nano Lett.* **2011**, *11* (7), 2919−2926.
(33) Xie, W.; Schlücker, S. Hot Electron-Induced Reduction of Small Molecules on Photorecycling Metal Surfaces. *Nat. Commun.* **2015**, *6*, 7570.
(34) Yan, X.; Wang, L.; Tan, X.; Tian, B.; Zhang, J. Surface-Enhanced Raman Spectroscopy Assisted by Radical Capturer for Tracking of Plasmon-Driven Redox Reaction. *Sci. Rep.* **2016**, *6*, 30193.
(35) Kim, Y.; Smith, J. G.; Jain, P. K. Harvesting Multiple Electron−hole Pairs Generated through Plasmonic Excitation of Au Nanoparticles. *Nat. Chem.* **2018**, *10* (7), 763−769.
(36) Brus, L. Noble Metal Nanocrystals: Plasmon Electron Transfer Photochemistry and Single-Molecule Raman Spectroscopy. *Acc. Chem. Res.* **2008**, *41* (12), 1742−1749.
(37) Boerigter, C.; Campana, R.; Morabito, M.; Linic, S. Evidence and Implications of Direct Charge Excitation as the Dominant Mechanism in Plasmon-Mediated Photocatalysis. *Nat. Commun.* **2016**, *7*, 10545.
(38) Boerigter, C.; Aslam, U.; Linic, S. Mechanism of Charge Transfer from Plasmonic Nanostructures to Chemically Attached Materials. *ACS Nano* **2016**, *10* (6), 6108−6115.
(39) Nicolai, S. H. de A.; Rodrigues, P. R. P.; Agostinho, S. M. L.; Rubim, J. C. Electrochemical and Spectroelectrochemical (SERS) Studies of the Reduction of Methylene Blue on a Silver Electrode. *J. Electroanal. Chem.* **2002**, *527* (1), 103−111.
(40) Nicolai, S. H. A.; Rubim, J. C. Surface-Enhanced Resonance Raman (SERR) Spectra of Methylene Blue Adsorbed on a Silver Electrode. *Langmuir* **2003**, *19* (10), 4291−4294.
(41) Joplin, A.; Hosseini Jebeli, S. A.; Sung, E.; Diemler, N.; Straney, P. J.; Yorulmaz, M.; Chang, W.-S.; Millstone, J. E.; Link, S. Correlated Absorption and Scattering Spectroscopy of Individual Platinum-Decorated Gold Nanorods Reveals Strong Excitation Enhancement in the Nonplasmonic Metal. *ACS Nano* **2017**, *11* (12), 12346−12357.
(42) Cleve, T. V.; Moniri, S.; Belok, G.; More, K. L.; Linic, S. Nanoscale Engineering of Efficient Oxygen Reduction Electrocatalysts by Tailoring the Local Chemical Environment of Pt Surface Sites. *ACS Catal.* **2017**, *7* (1), 17−24.
(43) Holewinski, A.; Xin, H.; Nikolla, E.; Linic, S. Identifying Optimal Active Sites for Heterogeneous Catalysis by Metal Alloys Based on Molecular Descriptors and Electronic Structure Engineering. *Curr. Opin. Chem. Eng.* **2013**, *2* (3), 312−319.

DOI: 10.1021/jacs.8b11949
J. Am. Chem. Soc. 2019, 141, 643−647